Volume 19
Number 10
December 2023
Pages 737–826

# Molecular Omics

rsc.li/molomics

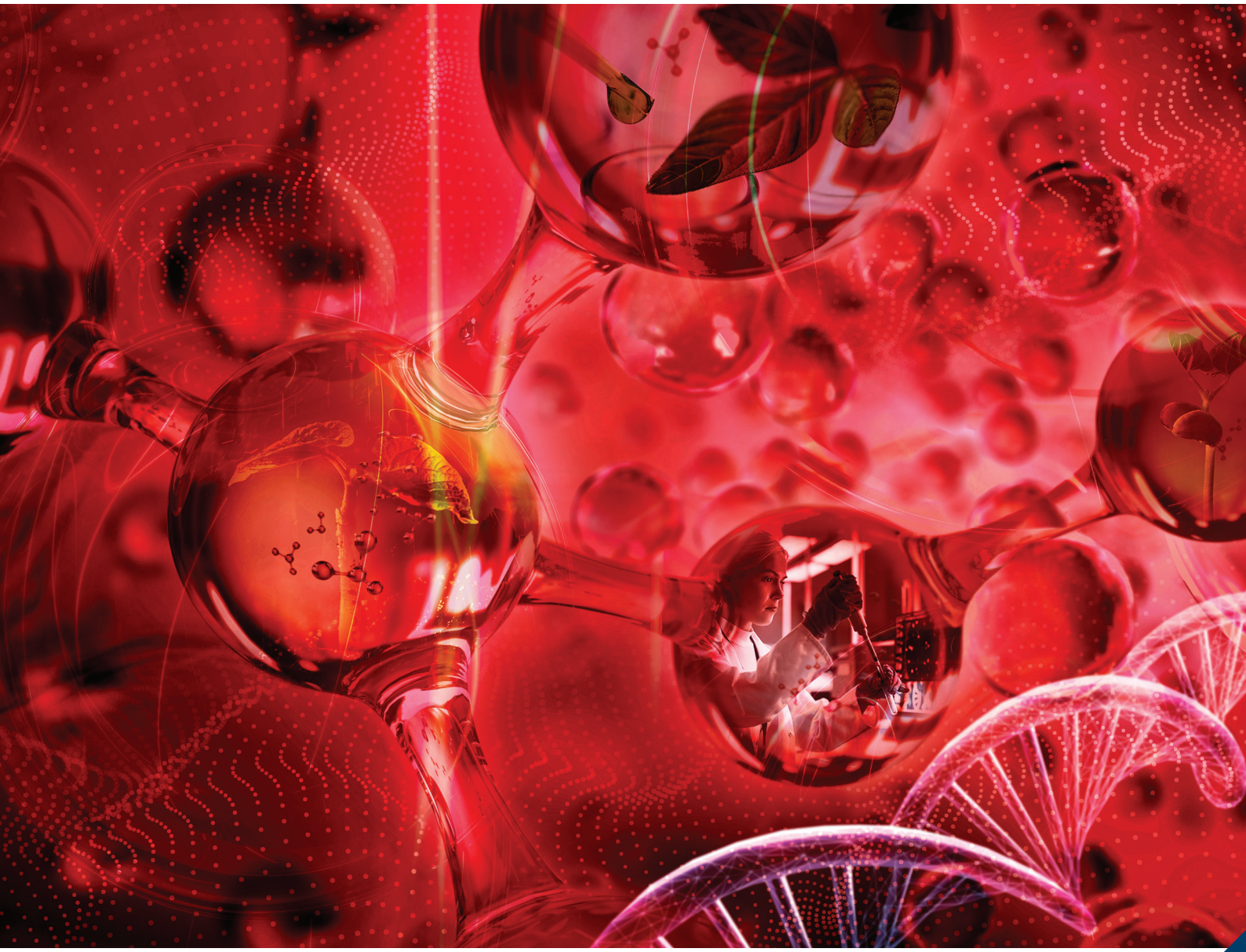

ISSN 2515-4184

**RESEARCH ARTICLE**
Taicia Pacheco Fill *et al.*
Metabolomic analysis reveals stress tolerance mechanisms in common bean (*Phaseolus vulgaris* L.) related to treatment with a biostimulant obtained from *Corynebacterium glutamicum*

ROYAL SOCIETY OF CHEMISTRY

Indexed in Medline!

Molecular Omics

ROYAL SOCIETY OF CHEMISTRY

RESEARCH ARTICLE

View Article Online
View Journal | View Issue



Cite this: *Mol. Omics*, 2023, 19, 743



# Metabolomic analysis reveals stress tolerance mechanisms in common bean (*Phaseolus vulgaris* L.) related to treatment with a biostimulant obtained from *Corynebacterium glutamicum*†

Stephanie Nemesio da Silva,[a] Luis Fernando de Oliveira,[a] Rodrigo Alberto Repke,[b] Alana Kelyene Pereira,[a] Luidy Darlan Barbosa,[a] Rafael Leiria Nunes,[b] Alessandra Sussulini,[a] Fabio Pinheiro[c] and Taicia Pacheco Fill*[a]

Received 27th May 2023,
Accepted 28th July 2023

DOI: 10.1039/d3mo00110e

rsc.li/molomics

Microbial biostimulants have emerged as a sustainable alternative to increase the productivity and quality of important crops. Despite this, the effects of the treatment on plant metabolism are poorly understood. Thus, this study investigated the metabolic response of common bean (*Phaseolus vulgaris*) related to the treatment with a biostimulant obtained from the extract of *Corynebacterium glutamicum* that showed positive effects on the development, growth, and yield of crops previously. By untargeted metabolomic analysis using UHPLC-MS/MS, plants and seeds were subjected to treatment with the biostimulant. Under ideal growth conditions, the plants treated exhibited higher concentration levels of glutamic acid, nicotiflorin and glycosylated lipids derived from linolenic acid. The foliar application of the biostimulant under water stress conditions increased the chlorophyll content by 17% and induced the accumulation of flavonols, mainly quercetin derivatives. Also, germination seed assays exhibited longer radicle lengths for seeds treated compared to the untreated control even in the absence of light (13–18% increase, $p$-value $<0.05$). Metabolomic analysis of the seeds indicated changes in concentration levels of amino acids (tryptophan, phenylalanine, tyrosine, glutamine, and arginine) and their derivatives. The results point out the enhancement of abiotic stress tolerance and the metabolic processes triggered in this crop associated with the treatment with the biostimulant, giving the first insights into stress tolerance mechanisms in *P. vulgaris*.

## 1. Introduction

Common bean (*Phaseolus vulgaris* L.) is one of the most consumed legumes in the world, playing a central role in food and nutrition security.[1] Currently, Brazil is one of the world's leading producers of the grain, whose production is aimed at domestic consumption.[2] It is estimated that more than 3.1 million tons of beans will be produced in the 2022 Brazilian harvest.[2] Dry bean grains are rich in proteins, fiber, unsaturated fatty acids (oleic, linoleic and α-linolenic acids), vitamins and minerals such as iron and potassium.[3,4] Furthermore, *P. vulgaris* is a source of polyphenolic compounds, mainly flavonoids, that play a key role in protecting against oxidative stress.[3]

Commonly, the increase in crop productivity is directly related to the use of synthetic chemical fertilizers and pesticides. Although these products have played a key role in the availability of food in the world, their prolonged use is associated with the development of insecticide resistance, soil degradation, pollution and eutrophication, in addition to all the risks related to human health.[5] In this regard, new practices, processes, and technologies have emerged taking into account a more sustainable and productive cultivation, consequently, with greater capacity for enhancing nutrition efficiency and stress tolerance.[5,6] For instance, an increase in crop resilience to environmental stress may help agricultural systems to overcome the negative effects of climate change.[7]

Economically attractive and operating sustainably, biostimulants have appeared in the global market increasing the quality of yields and maintaining ecological balance.[8,9] This segment had a turnover of US$ 3.5 billion in 2022 and has an estimated growth projection of US$ 6.2 billion by 2027.[10] Plant biostimulants are complex products of biological origin whose main function is to stimulate natural processes of the plant that

[a] *Instituto de Química, Universidade Estadual de Campinas;, Campinas, São Paulo, 13083-970, Brazil. E-mail: taicia@unicamp.br; Tel: +55-19-35213092*
[b] *Tradecorp do Brasil Ltda, Campinas, São Paulo, 13190-000, Brazil*
[c] *Instituto de Biologia, Universidade Estadual de Campinas, Campinas, São Paulo, 13083-862, Brazil*

† Electronic supplementary information (ESI) available. See DOI: https://doi.org/10.1039/d3mo00110e

benefit it,[9] mainly nutrient use efficiency and tolerance to environmental stress, improving crop growth and productivity.[11] Often, microbial biostimulants are related to extracts of microorganisms, thus consisting of a wide range of bioactive compounds acting on different stages of plant development.[12]

The bioactive compounds produced by microorganisms are able to modulate the plant's physiological responses in order to protect and directly or indirectly stimulate its development.[13] In particular, specialized metabolites upregulate the expression of antioxidant enzymes of the plant, induce systemic resistance and the biosynthesis of photosynthetic pigments (*i.e.* carotenoids, anthocyanins, and flavonoids).[14–16] This is able to increase plant growth and resistance to different abiotic stresses, such as drought and salinity, and biotic stresses, related to insect and phytopathogen attacks.[13,17]

Since its discovery and isolation in the 1950s, the Gram-positive bacterium *Corynebacterium glutamicum* has been explored in the industrial sector,[18] often applied for the bioproduction of amino acids such as L-glutamic acid and 5-aminolevulinic acid.[19] In agriculture, exogenous supplementation of these compounds can be used to improve productivity and resistance to various abiotic stresses, which are considered promising products for crop nutrition and yield.[20,21] The Vorax™ biostimulant (Tradecorp do Brasil Ltda), also known as Biimore™ or Quikon™ worldwide, is based on an extract from the fermentation of the bacterium *C. glutamicum* MQ06 in sugarcane molasses using an exclusive process. Due to its high complexity, the total chemical composition is still unknown. The constituents determined are concentrated in amino acids (28.6%), carbohydrates (18.4%), and vitamins (0.1%). Among amino acids, the highest percentage is L-glutamic acid (25.6%). Although some studies demonstrate the positive effect of Vorax™ treatment in several crops,[22,23] the effects of this biostimulant in the plant metabolome remained unknown.

In the present study, modulations in *Phaseolus vulgaris* metabolism related to the treatment with the Vorax™ biostimulant under ideal and abiotic stress conditions and at different stages of plant development were investigated. Untargeted metabolomics was applied using UHPLC-MS/MS in association with multivariate statistical analysis and molecular networking tools. Variations were detected in the concentration level of lipids, amino acids and specialized metabolites such as flavonoids and coumarins, indicating the induction of particular biosynthetic pathways due to the plant–biostimulant interaction.

# 2. Experimental

## 2.1 Biostimulant composition and the treatment method

The Vorax™ biostimulant was kindly provided by Tradecorp do Brasil Ltda (Campinas, São Paulo, Brazil). This biostimulant is an extract obtained from the exclusive fermentation of the bacterium *C. glutamicum* MQ06 in sugarcane molasses and contains a complex composition including amino acids (28.6%), carbohydrates (18.4%), and vitamins (0.1%). The *C. glutamicum* strains are deposited at the Centro Pluridisciplinar de Pesquisas Químicas, Biológicas e Agrícolas (CPQBA). Vorax™ was used according to the manufacturer's instructions. Plants were subjected to the manual nebulization of 1% v/v aqueous solution of the biostimulant (treated) or sterile water (untreated) at a rate of 50 mL $ha^{-1}$ using a spray bottle. This procedure was performed only once. After 72 h of nebulization, the leaves were collected, immediately immersed in liquid nitrogen and then stored at −80 °C until sample extraction. The collected time was selected according to the previous study.[24]

## 2.2 Treatment effect of Vorax™ on plant metabolome

Common beans (*P. vulgaris* L., genotype IPR-139) seeds of the 2017/2018 season were provided by Tradecorp do Brasil Ltda (Campinas, São Paulo, Brazil). The genotype grew in 8 L capacity pots, containing the Vidaverde™ (Mogi Mirim, São Paulo, Brazil) substrate enriched with 2 L of Vithal™ (Itaim Bibi, São Paulo, Brazil) aqueous solution composed of 1.8% N, 1.8% P; 7.2% K, 0.05% Fe and 0.002% Mo. The experiment was carried out in a greenhouse at Escola Superior de Agricultura Luiz de Queiroz (Piracicaba, São Paulo, Brazil) under a 11 h/13 h light/dark photoperiod, in the average temperature range of 26–36 °C, and the maximum water field capacity up to the vegetative stage R1.[25] Plants were divided into two groups: (C) control (untreated) and (T) treated (treated with Vorax™). For each group, five individual plants were selected randomly. The leaves of the first trefoil were used to generate a single extract. The sample preparation was performed in triplicate.

## 2.3 Plant treatment with the biostimulant under water stress conditions

For the evaluation of treatment with Vorax™ under water stress conditions, an assay was performed according to the scheme presented in Table 1. The growth of the genotype was conducted in a greenhouse at Universidade Estadual de Campinas (Campinas, São Paulo, Brazil) in the average temperature range of 21–37 °C and 13/11 h light/dark photoperiod until the collection of leaves. Seeds were sown directly to soil (potting compost) under the same nutritional conditions as in topic 2.2. Treated plants received the foliar application of Vorax™. The plants subjected to water stress suffered from the total absence of irrigation for 7 days, with soil humidity decreasing from 60 (±0.8)%, with regular irrigation, to 33 (±0.4)% at peak stress. This period of stress was selected by evaluating the plant integrity limit through physiological aspects. The humidity in the pots was determined by collecting mass samples in Petri dishes at these two times, drying in an oven at 60 °C for 72 h and calculating the difference in mass related to water. Eight individual plants were selected randomly for each group: Vorax™ Treatment after water stress (WST), untreated water

Table 1 Study design used to evaluate Vorax™ treatment under water stress conditions

| Trial | Day 0 | Day 7 | Day 10 |
|---|---|---|---|
| WST | Water stress | Vorax™ treatment | Sample collection |
| WS | Water stress | Untreated | Sample collection |
| NSNT | No stress | Untreated | Sample collection |

 

stress (WS) and No water stress or treatment (NSNT). The leaves of the first trefoil were used to generate the extract. The sample preparation was performed in duplicate. The chlorophyll content in the leaves at different times (0 days, 7 days, 10 days) was measured using a digital chlorophyll meter (Falker, Brazil) in six different plants for each group.

### 2.4 Germination assays

*Phaseolus vulgaris* seeds were surface-sterilized using a 5% sodium hypochlorite for 2 min and rinsed with distilled water for 2 min. The seeds were incubated on germitest paper (CIENLAB, Brazil) in Petri dishes (diameter 8.5 cm) using six seeds per plate. Five repeats were performed. A total of 6 mL of Vorax™ aqueous solution (500 ppm) was applied to the surface of each plate. Deionized water was used as a negative control and glyphosate herbicide solution (1%, w/w) was used as a positive control. The plates were incubated at 25 °C in the total absence of sunlight (−) or in a 12 h/12 h day/night photoperiod (+) for 7 days. After the incubation time, the radicle length was measured using ImageJ software (**https://imagej.net/Welcome**). The average radicle length ± SE (standard error) of treated seeds with Vorax™, positive control and negative control of the light and dark assays were calculated. Of the six seeds contained in each plate, two were excluded from the analysis: those with the highest and the lowest/no radicle growth.

### 2.5 Metabolite extraction

The leaves of the first trefoil from each selected plant were macerated together under liquid nitrogen. Then, about 100 mg of plant material were transferred to a 2 mL glass vial and 1 mL of methanol with formic acid (0.1%, v/v, cold) was added. The mixture was sonicated for 60 min in an ultrasound bath and centrifuged at 16 200*g* for 3 min at 4 °C. Supernatants were filtered through a 0.22 μm PTFE hydrophobic membrane filter, dried using a speed vacuum concentrator for 90 min at 30 °C and stored at −20 °C until analysis.

For germinated seed extraction, three solvent mixtures were tested: mixture 1 (7 : 3, methanol : water, v/v), mixture 2 (3 : 1 : 1, chloroform : methanol : water, v/v) and mixture 3 (8 : 2, methanol : water with 0.1% formic acid, v/v) according to Silva *et al.*, 2020[26] and Almeida Trapp *et al.*, 2014[27] with some modifications. All seeds in a plate were macerated together under liquid nitrogen, and about 100 mg of the plant material was extracted using 1 mL of the cold solvent mixture (1, 2 or 3). Subsequently, the solution was subjected to ultrasound bath treatment, centrifugation, filtration and concentration as described. The extraction procedures were performed in duplicate for each solvent system.

The composition of Vorax™ was also investigated to ensure that the metabolic changes detected were related to plant metabolism and not due to the accumulation of compounds present in the biostimulant. For this, aqueous solution of Vorax™ (1%, v/v) was prepared using ultrapure water. The solution was centrifuged at 16 200 *g* for 5 min at 25 °C and the supernatant was filtered straight into a vial using a 0.22 μm PTFE hydrophobic membrane filter. This procedure was performed in duplicate.

### 2.6 Metabolomic profile by liquid chromatography-mass spectrometry

The samples were prepared by resuspending the plant extracts in 1 mL of methanol and diluting 100 μL of this solution with 900 μL of methanol in a vial. Ultra-high performance liquid chromatography (UHPLC) analysis was performed using an Ultimate 3000 instrument coupled to a Q Exactive Plus Hybrid Quadrupole-Orbitrap Mass Spectrometer (Thermo Fisher Scientific, USA) equipped with a heated electrospray ionization (HESI-II) probe. Chromatographic separation was performed using a reversed-phase Accucore C18 column (Thermo Scientific, USA, 2.6 μm, 2.1 × 100 mm) at a flow rate of 0.3 mL $min^{-1}$ with the mobile phases A (water containing 0.1% formic acid, v/v) and B (acetonitrile) eluted in the gradient: 0–10 min, 5% to 98% B; 10–17 min, 17–17.01 min, 98 to 5% B; 17.01–25 min, 5% B for leaf samples or 0–10 min, 5% to 98% B; 10–20 min, 98% B; 20–21.2 min, 98 to 5% B and 21, 2–30 min, 5% B at 45 °C for seed samples. The injection volume was 3 μL.

Detection was performed in the positive-ion mode over a range of *m/z* values of 115 to 1500 with an acquisition rate of 10 Hz, normalized collision energy (NCE) of 30 eV and the following main parameters: nebulizing gas temperature of 250 °C with a flow of 10 L $min^{-1}$, nebulization gas pressure: 45 psi and capillary voltage: +3500 V, with a potential plate end of −500 V. The 6 most intense ions per cycle were selected for automatic fragmentation (Data dependent MS/MS). The data were acquired and processed using Xcalibur software version 3.0.63 (Thermo Fisher Scientific, USA). All samples were analyzed in random order. To monitor the accuracy and stability of the analytical method, a quality control (QC) sample, prepared by collecting equivalent volumes (10 μL) of each sample in the same vial, was injected three times at the beginning of the batch, after five samples and at the end of the injections.[28]

### 2.7 Statistical analysis

Statistical analyses of the germinated seed radicle length and chlorophyll content data were performed using Action Stat 4.0 software (**https://www.actionstat.com.br**). After the Shapiro–Wilk test for normality, statistical differences between three or more means were calculated by one-way analysis of variance (ANOVA) or the Kruskal–Wallis test. Student's *t*-test of homogeneous or heterogeneous variance was applied to compare two means after the *F* test. Data are expressed as means ± standard deviation (SD) and statistically significant differences between treatments were considered corresponding to a $p$-value $< 0.05$.

The raw files obtained after UHPLC-MS/MS analysis were converted to mzXML format using the MSConvertGUI tool from ProteoWizard software (Proteowizard Software Foundation, USA) and pre-processed using the MZmine 2.53 package[29] according to parameters shown in Table A.1 (ESI†). Then, multivariate and univariate statistical analyses, including principal component analysis (PCA) and partial least squares-discriminant analysis (PLS-DA), were carried out by the MetaboAnalyst 4.0 platform[30]

with the removal of features with at least 50% missing values and estimation of remaining missing values using the KNN algorithm. Additionally, feature filtering with RSD (relative standard deviation) >30% in the QC samples, normalization by the median and data scaling by the Pareto scaling method were performed. To screen out significant differential metabolites, it was considered variable importance in the projection (VIP) score value of the first principal component in the PLS-DA ≥2.5 and *p*-value <0.05 using the *t*-test. The reliability of the PLS-DA model was verified using a permutation test (cross-validation).

### 2.8 Molecular networking and metabolite annotation

Based on spectra similarity, molecular networks and dereplication of MS/MS data were carried out through the global natural products social molecular networking (GNPS) online platform.[31] For this, a metadata table in.txt format, discriminating the samples by group, the .mgf and.csv files, generated from the pre-processing of MS/MS data in MZmine 2.53 software, were uploaded to the GNPS and molecular networking was created using the feature based molecular networking (FBMN) tool.[32] The FBMN job links are available at **https://gnps.ucsd.edu/ProteoSAFe/status.jsp?task=30b4c286b13f443fb03fa2722c68aa94(topic3.1)**, **https://gnps.ucsd.edu/ProteoSAFe/status.jsp?task=e97e6ce296d94bec9ce080cfffe65e81** (topic 3.2) and **https://gnps.ucsd.edu/ProteoSAFe/status.jsp?task=5ef66c81a1874992b53eebb33e5aea3a** (topic 3.3). The results were obtained considering the precursor ion mass tolerance and fragment ion mass tolerance of ±0.01 Da, cosine score above 0.7 and minimum 4 matched peaks to assist the metabolomics annotation. Moreover, experimental MS/MS spectra were compared with GNPS spectral libraries using the same parameters. The output of the molecular network was visualized and edited using Cytoscape version 3.7.2 (Cytoscape Consortium, San Diego, USA). The nodes correspond to ion features while the edges between the nodes represent the MS/MS cosine score. The pie charts inside the node represent the relative abundance of the feature in the samples of the analyzed groups.

## 3. Results

### 3.1 Treatment with Vorax™ causes variation in *P. vulgaris* metabolism

To investigate the effect of Vorax™ treatment on *P. vulgaris* metabolism, leaf extracts of the treated and control plants were evaluated by ultra-high-performance liquid chromatography tandem mass spectrometry (UHPLC-MS/MS). In order to provide an overview of the data, principal component analysis (PCA) was performed. According to the PCA scores plot in Fig. 1A, the first two principal components, which were responsible for 49.7% (29.9% for PC1 and 19.8% for PC2) of the overall data variance, exhibit a separation tendency between non-treated (Control) and treated with Vorax™ (Treated) samples. While samples from the control group are distributed along PC1, treated samples exhibit variation in PC2. The separation between groups is clearer by the supervised method of partial least squares-discriminant analysis (PLS-DA), which is presented in Fig. S1 (ESI†). The reproducibility of the instrumental system was assessed by the pooled analysis of the quality control (QC) samples. The tight clustering of the pooled QCs in the PCA scores plot demonstrated the stable performance of the instrument. The validation of the PLS-DA classification model was performed by cross-validation with the coefficient of determination $R^2$ = 0.94 and prediction degree $Q^2$ = 0.72, indicating the high reliability of the model.

Among the metabolite features classified as statistically significant by the *t*-test, four were annotated based on analysis of accurate mass (errors ranged from 0 to 5 ppm) and MS/MS fragmentation profile by means of databases, corresponding to level 2 of identification according to the Metabolomics Standards Initiative (MSI).[33] The compounds annotated were glutamic acid (*m/z* 148.0605, *p*-value = $2.12 \times 10^{-6}$), nicotiflorin (*m/z* 595.1658, *p*-value = 0.03), 1-linolenoylglycerol (*m/z* 353.2687, *p*-value = $1.46 \times 10^{-5}$) and 1-linolenoyl-3-galacto-pyranosylglycerol (*m/z* 532.3483, *p*-value = $2.63 \times 10^{-5}$). All of them were detected with higher signal intensities in the samples of the treated group (Fig. 1B).

The MS/MS spectra of glutamic acid at $[M + H]^+$ *m/z* 148.0605 (Fig. S2, ESI†) display the ion corresponding to a neutral water loss $[M - H_2O + H]^+$ at *m/z* 130.0500, the immonium ion $[M - CO_2H_2 + H]^+$ at *m/z* 102.0553, and the product ion at *m/z* 84.0449, corresponding to the loss of $H_2O$ from the immonium ion $[M - CO_2H_2 - H_2O + H]^+$.[34,35] Additionally, the nicotiflorin MS/MS spectrum with $[M + H]^+$ at *m/z* 595.1658 (Fig. S3, ESI†) presents a base peak at *m/z* 287.0549, characteristic of the aglycone backbone of kaempferol $[A + H]^+$, a low intensity signal at *m/z* 449.5047, referring to the monoglycosylated aglycone $[A + 162 + H]^+$, and disaccharide fragment ions at *m/z* 129.0548, *m/z* 85.0289 and *m/z* 71.0497.[36,37]

In the case of the compound 1-linolenoylglycerol with $[M + H]^+$ at *m/z* 353.2687, the MS/MS spectrum (Fig. S4, ESI†) displays the main fragments at *m/z* 67.0548, *m/z* 81.0704, *m/z* 95.0858, *m/z* 109.1014, and *m/z* 149.1326 that characterize alkyl chain fragmentation of the monoacylglycerol fatty acid with 18 carbons and 3 unsaturations. It is also observed a base peak at *m/z* 261.2219 refers to the neutral loss of glycerol $[M + H - C_3H_8O_3]^+$ by inductive cleavage.[38] A similar MS/MS spectrum is observed for the 1-linolenoyl-3-galacto-pyranosylglycerol with $[M + NH_4]^+$ at *m/z* 532.3482 (Fig. S5, ESI†). One of the main fragments is the *m/z* 353.2676, referring to the neutral loss of a pyranose fragment ($C_6H_{10}O_5$), equivalent to the protonated 1-linolenoylglycerol molecule. The base peak at *m/z* 261.2212 corresponds to the glycerol loss, and alkyl chain fragments at *m/z* 95.0859, *m/z* 109.1013 and *m/z* 159.1169.

The MS/MS data were also submitted to molecular networking analysis through the feature based molecular networking (FBMN) tool at the global natural products social molecular networking (GNPS) platform. It was observed two spectral families with concentration level variation of metabolites (node) between control and Vorax™-treated groups. According to the spectral similarity of the metabolites in Fig. 1C, it was possible to annotate the compound at *m/z* 694.4003 as gingerglycolipid A (Fig. S6, ESI†), derived from linolenic acid as well as the metabolites with precursor ions at *m/z* 353.2687 and *m/z* 532.3482. All these three

 

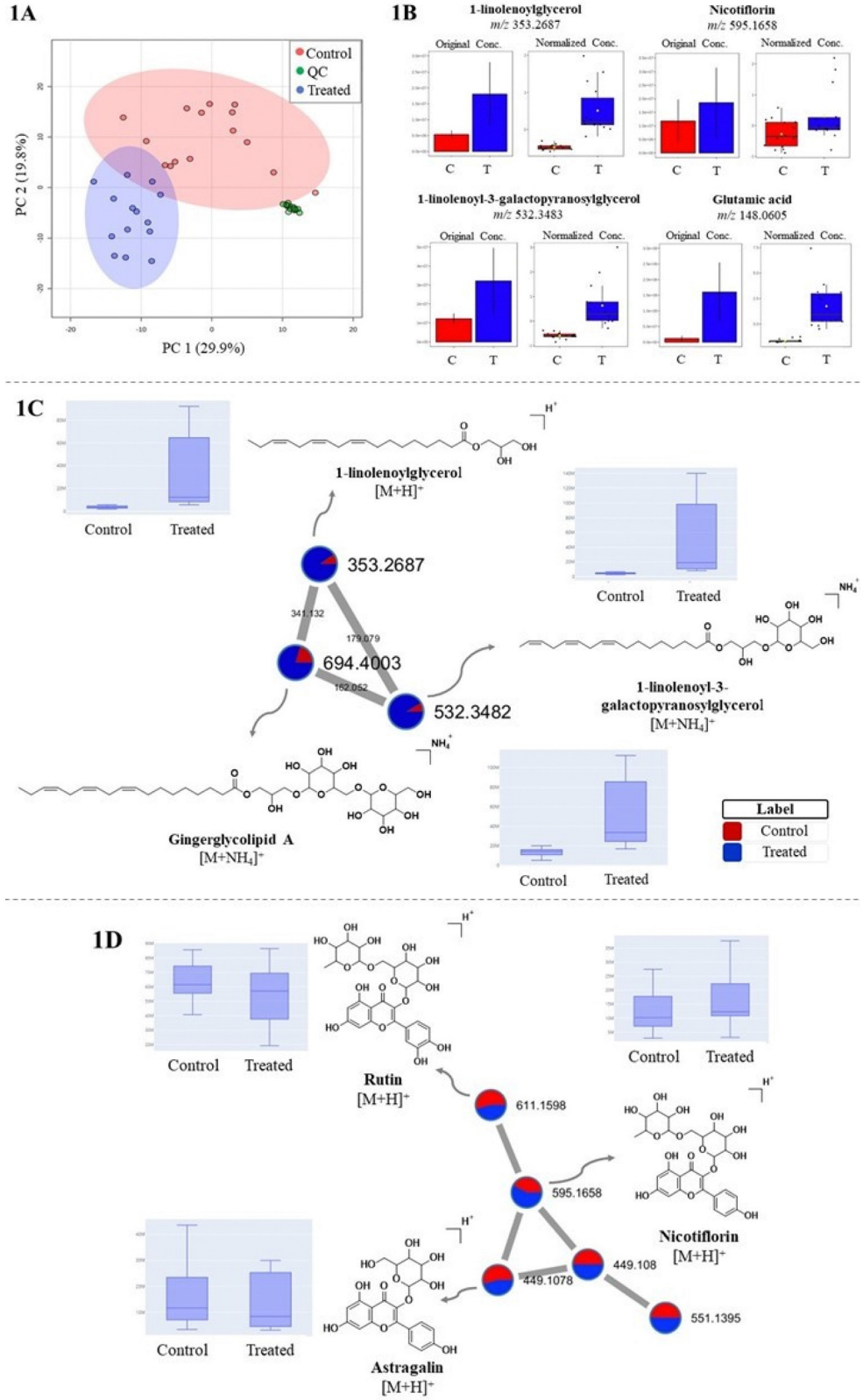


Fig. 1 (A) PCA scores plot of data acquired by UHPLC-MS/MS of leaf extracts from non-treated (C) and Vorax™-treated (T) samples with $n$ = 5 (three repetitions). (B) Boxplot of differential metabolites between the groups obtained from MetaboAnalyst. Spectral family of (C) lipids and (D) flavonoids obtained by feature based molecular networking of MS/MS data of leaf extracts from *Phaseolus vulgaris* Vorax™-treated (T) and non-treated (C) samples. The metabolites were annotated manually through accurate mass and fragmentation pattern analysis. Boxplot next to the metabolite displays its relative concentration based on the peak intensity in each group.

annotated glycerolipids exhibited higher concentration levels for samples from the treated group. To the flavonoids spectral family in Fig. 1D, rutin (*m/z* 611.1598) and astragalin (*m/z* 449.1078) showed lower concentration levels in the treated group while nicotiflorin (*m/z* 595.1658) exhibited increased concentration level in leaf samples treated with the biostimulant, corroborating the result obtained in the statistical analysis. The astragalin (*m/z* 449.1078, Fig. S7, ESI†) and rutin (*m/z* 611.1598, Fig. S8, ESI†) were annotated by comparison of MS/MS spectra with the GNPS databases.

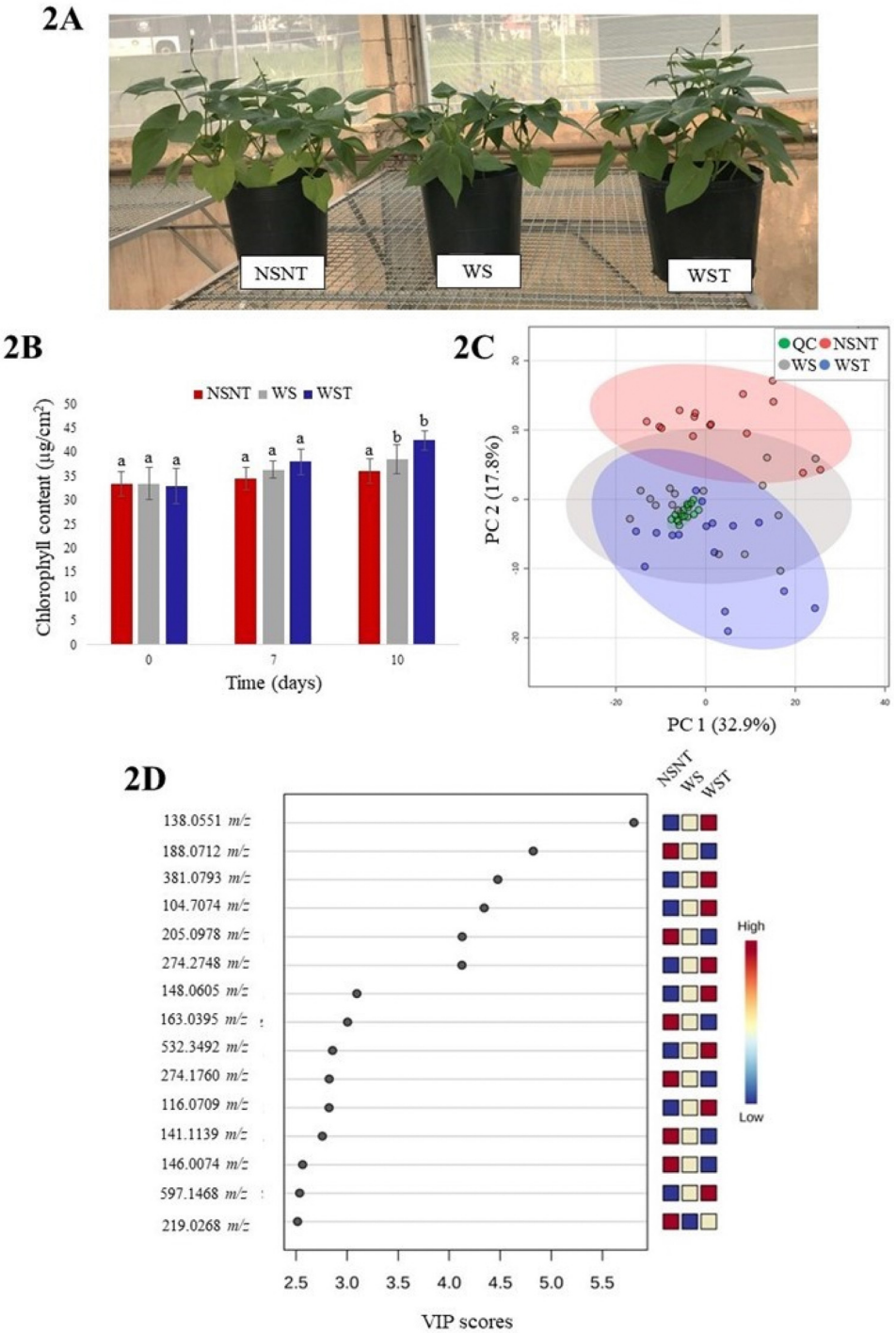


Fig. 2 (A) Comparison between pots of NSNT (no water stress or treatment), WS (untreated water stress), and WST (Vorax™ treatment after water stress) after 10 days. (B) Chlorophyll content by the time. Values are the mean of six replicates ± standard deviation (±SD). Different letters (a) and (b) indicate statistically significant differences between trials ($p$-value $<0.05$). (C) PCA scores plot of data acquired by UHPLC-MS/MS, positive mode, of leaf extracts samples from WST, WS and NSNT with $n = 8$ (two repetitions). (D) Contribution of the first 15 variables in the projection (VIP scores) of the PLS-DA model.

 

All discussed metabolites were not detected in the biostimulant samples, except glutamic acid (Table A.2, ESI†). The low amount of Vorax™ applied, 50 mL per hectare of a 1% (v/v) aqueous solution, indicates that the variation in the level of glutamic acid between the groups is due to changes in the plant's metabolism and not due to the Vorax™ composition itself.

### 3.2 Increased tolerance to water stress due to treatment with Vorax™

After evaluating the effect of biostimulant treatment under ideal growing conditions, we asked if the positive effect would be potentiated under stress conditions. Therefore, an assay was conducted submitting *P. vulgaris* to the absence of irrigation for 7 days, and then, treating with Vorax™ 3 days before collection. Morphological analysis comparing plots of WST (Vorax™ treatment after water stress), WS (untreated water stress) and NSNT (no water stress or treatment) at day 10 showed greater development and lower incidence of stoma closure for WST (Fig. 2A). The analysis of the chlorophyll content exhibited a significant increase of WST (42.47 μg $cm^{-2}$) in relation to WS (38.50 μg $cm^{-2}$), $p$-value = 0.045, and in relation to NSNT (36.15 μg $cm^{-2}$), $p$-value = 0.002 (Fig. 2B).

To investigate metabolomic profile variations, multivariate analysis of the UHPLC-MS/MS data was performed. The first two principal components of the PCA scores plot (Fig. 2C) were responsible for 50.7% of the total variance (32.9% for PC1 and 17.8% for PC2), showing a clear tendency of separation of the NSNT in relation to WS and WST. This indicates a characteristic metabolic profile for NSNT samples. The tight clustering of the pooled QCs in the PCA indicated the stable performance of the UHPLC-MS/MS system. Beyond the prominent separation of NSNT in relation to WS and WST, the PLS-DA scores plot (Fig. S9, ESI†) exhibits a relative separation between WS and WST, pointing to differences in metabolic profiles of these trials. Validation of the PLS-DA model presented $R^2$ = 0.89 and $Q^2$ = 0.79, showing that the proposed classification model is valid to differentiate the studied groups.

The relevance of each feature in the separation of the PLS-DA model was evaluated through the variable importance in projection (VIP) scores. Fig. 2D presents the 15 differential features (VIP ≥ 2.5) obtained in the analysis. Metabolites were annotated by accurate mass analysis, MS/MS spectra or as a hit in the GNPS database (Fig. S10, ESI†). The amino acid glutamic acid with $[M + H]^+$ at $m/z$ 148.0605, the lipid 1-linolenoyl-3-galactopyranosyl glycerol $[M + NH_4]^+$ ($m/z$ 532.3492) and the flavonoid quercetin-3-*O*-xylopyranosyl(1 → 6)-glucopyranoside $[M + H]^+$ ($m/z$ 597.1468) presented an increase in their concentration levels in the two trials subjected to water stress, but a more expressive induction in WST samples (Fig. S11, ESI†). In contrast, the amino acid tryptophan ($[M + H - NH_3]^+$ $m/z$ 188.0712; $[M + H]^+$ $m/z$ 205.0978) and the compound 7-hydroxycoumarin $[M + H]^+$ $m/z$ (163.0394) exhibited higher concentration levels in the NSNT samples compared to WST and WS (Fig. S12, ESI†) treatments. These results indicate changes in the pathway of these metabolites either by water stress or a combination of stress and treatment with Vorax™.

Additionally, the data were also analyzed by the FBMN tool. It was observed a flavonoid spectral family (Fig. 3) with the accumulation of several glycosylated flavonols in the WST (blue) compared to WS (grey) and NSNT (red), mainly quercetin derivates: rutin $[M + H]^+$ ($m/z$ 611.1624), quercetin-3-xylosyl-(1 → 2) arabinofurnoside $[M + H]^+$ ($m/z$ 567.1360), hyperoside $[M + H]^+$ ($m/z$ 465.1045), isoquercetin $[M + H]^+$ ($m/z$ 465.1044) and quercetin-3-*O*-xylopyranosyl-(1 → 6)-glucopyranoside $[M + H]^+$ ($m/z$ 597.1461), which was considered statistically significant by PLS-DA analysis (VIP score = 2.6). Only astragalin $[M + H]^+$ ($m/z$ 449.1087) showed a higher concentration level in WS compared to the other trials. The metabolites were annotated by comparing the experimental MS/MS data with the GNPS library spectral database, manual verification of fragmentation pattern, and comparison to previous studies. The accurate mass measurements, mass errors, ion formula, retention time and MS/MS fragments are presented in Table 2.

The discussed metabolites were not detected in the biostimulant samples (Table A.2, ESI†), except glutamic acid. Variations in glutamic acid levels detected between the NSNT and WS groups (absent of Vorax™ treatment) reinforce that the increase in the relative abundance of this metabolite in the WS and WST groups is due to changes in the plant's metabolism.

### 3.3 Vorax™ improves seed development

In order to evaluate the biostimulant influence in the initial stages of plant development, *P. vulgaris* seeds were treated with Vorax™ and compared to water (negative control) and glyphosate herbicide (positive control) treated seeds. Moreover, abiotic stress caused by the total absence of light was also measured.

After the germination period, the radicle length was used as a growth parameter (Fig. S13, ESI†). Higher average radicle lengths were obtained for seeds treated with Vorax™ in relation to the control in both assays, with exposure for a photoperiod of 12 h/12 h light/dark (+) and complete absence of light (−), graphically represented by the boxplot in Fig. 4A and B, respectively. In the ANOVA test for the (+) data, normal distribution, and in the Kruskal–Wallis test for the (−) data, non-normal distribution, the difference observed between Vorax™ and negative control treatments was considered statistically significant ($p$-value < 0.05). Such a result is an indication that even in early stages the biostimulant can act pronounced, especially when abiotic stress conditions are applied, in this case, the total absence of luminosity.

Metabolite extraction procedures of *P. vulgaris* seeds with different solvent mixtures were used to evaluate the amount and diversity of metabolite annotations. According to the Venn diagram (Fig. 4C), a total of 219 metabolites were recorded by the GNPS spectral libraries for the three extractor solvent mixtures. Of those, 124 were extracted in mixture I (56.6% of the total), 128 in mixture 2 (58.4% of the total), and the highest quantities in mixture 3, 154 (70.3% of the total). Furthermore, greater chemical diversity was also observed for extractor solvent mixture 3, with exclusive annotation of 45 metabolites. From these results, the data acquired using mixture 3 as the extracting solvent were selected for subsequent analysis.

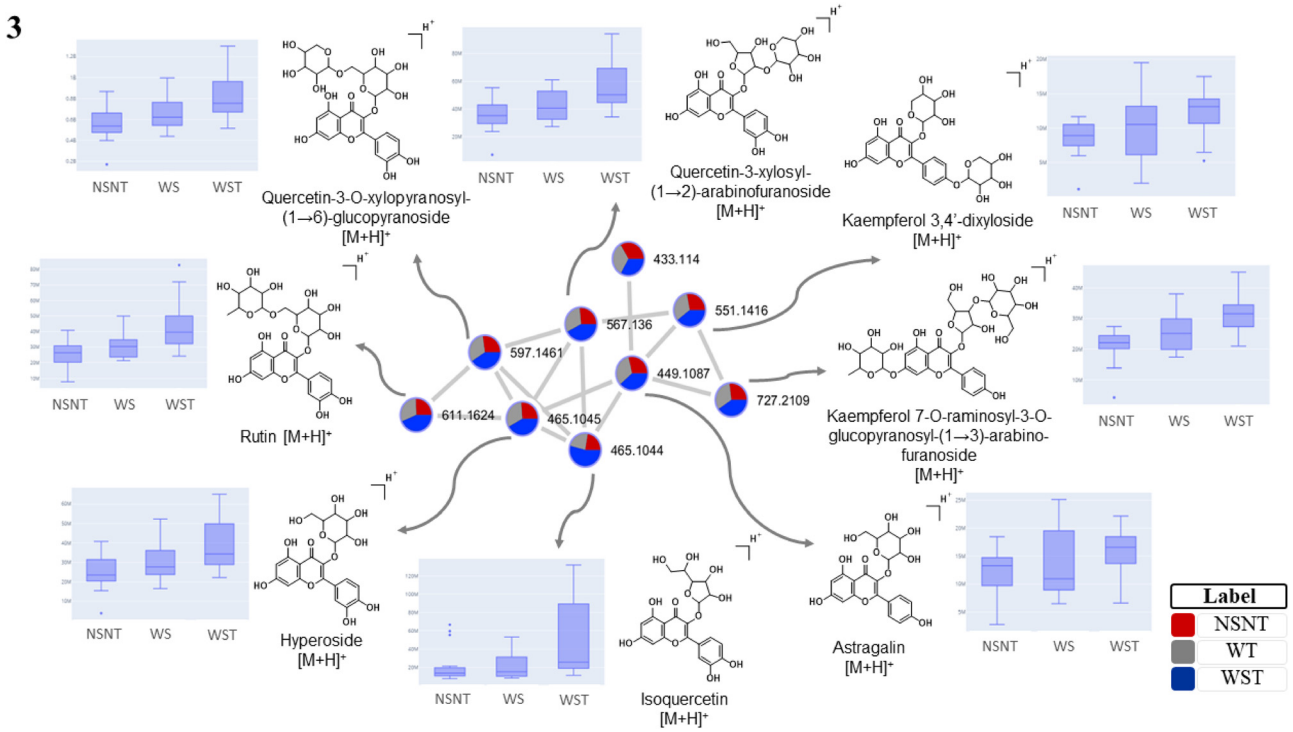


Fig. 3 Spectral family of flavonoids obtained by feature based molecular networking (FBMN) for the MS/MS data of leaf extracts of *P. vulgaris* in WST (Vorax™ treatment after water stress), WS (untreated water stress) and NSNT (no water stress or treatment) trials. The metabolites were putatively identified through dereplication data using the GNPS database. Boxplot next to each metabolite displays its relative concentration level in each group.

The influence of the biostimulant treatment on the *P. vulgaris* seeds metabolism was evaluated by multivariate statistical analysis. In the 2D PCA score plot (Fig. 4D), there is a tendency of separation per assay between the samples. While (+) data ranged along the positive direction of PC1 and PC2, (−) data were distributed mainly in the negative direction of PC1. The first two principal components were responsible for 58.5% of the overall data variance (29.5% for PC1 and 16.1% for PC2). For the PLS-DA analysis (Fig. S14, ESI†), validation of the model by cross-validation presented $R^2$ = 0.76 and $Q^2$ = 0.23 for the data of the (+) and (−) assays. Moreover, the PLS-DA model of the (+) data exhibited $R^2$ = 0.91 and $Q^2$ = 0.27 while the PLS-DA of the (−) data presented $R^2$ = 0.94 and $Q^2$ = 0.56, showing that the proposed classification model is valid to differentiate the studied groups.

From the VIP scores of PLS-DA, differential features (VIP score ≥2.5) were determined between positive control and treated groups of each assay. Metabolites were annotated through accurate mass and fragmentation pattern manual analysis or MS/MS comparison with the GNPS library. Upon exposure for a photoperiod of 12 h/12 h light/dark (+), an increase in the levels of tryptophan $[M + H]^+$ (*m/z* 205.0971) and 2-hydroxy-9-oxo-octadecatrienoic acid $[M + H]^+$ (*m/z* 309.2060) beyond a decrease of glutamine $[M + H]^+$ (*m/z* 147.0760), arginine $[M + H]^+$ (*m/z* 175.1187) and the fatty acid linolenic acid $[M + H]^+$ (*m/z* 279.2310) were obtained in the samples from the Vorax™-treated group (Fig. 4E). Already for the VIP scores of the complete absence of sunlight (−) data (Fig. 4F), all of the annotated metabolites showed accumulation in the treated group:

Table 2 Flavonoids annotated by FBMN with different concentration levels between WST, WS and NSNT groups

| Predicting compound | PubChem CID | Ion formula $[M + H]^+$ | RT (min) | Calc. *m/z* | Exp. *m/z* | Mass error (ppm) | MS/MS |
|---|---|---|---|---|---|---|---|
| Kaempferol 7-*O*-raminosyl-3-*O*-glucopyranosyl-(1 → 3) arabino-furanoside | 51 136 541 | $C_{32}H_{39}O_{19}$ | 2.91 | 727.2080 | 727.2099 | 2.61 | 440.8534, 287.0556, 225.0764, 129.0546, 85.0291, 71.0499 |
| Quercetin 3-*O*-xylopyranosyl-(1 → 6)-glucopyranoside | 5 315 208 | $C_{26}H_{29}O_{16}$ | 2.85 | 597.1450 | 597.1468 | 2.98 | 562.2053, 303.0504, 97.0290, 85.0289, 73.0291 |
| Astragalin | 5 282 102 | $C_{21}H_{21}O_{11}$ | 3.08 | 449.1078 | 449.1089 | 2.41 | 381.8889, 287.0556, 167.0347, 149.0235, 85.0291 |
| Hyperoside | 5 281 643 | $C_{21}H_{21}O_{12}$ | 2.86 | 465.1028 | 465.1042 | 3.16 | 303.0504, 291.3327, 176.9907, 97.0290, 85.0291 |
| Isoquercetin | 5 280 804 | $C_{21}H_{21}O_{12}$ | 3.13 | 465.1028 | 465.1042 | 3.16 | 395.6780, 303.0503, 182.0669, 97.0290, 85.0290 |
| Kaempferol 3,4'-dixyloside | 44 258 938 | $C_{25}H_{27}O_{14}$ | 3.34 | 551.1395 | 551.1414 | 3.32 | 351.8049, 287.0555, 242.7833, 97.0291, 73.0291 |
| Quercetin 3-xylosyl-(1 → 2) arabinofuranoside | 44 259 231 | $C_{25}H_{27}O_{15}$ | 3.09 | 567.1344 | 567.1362 | 3.14 | 483.3628, 303.0505, 115.0395, 97.0291, 73.0292 |
| Rutin | 5 280 805 | $C_{27}H_{31}O_{16}$ | 2.99 | 611.1607 | 611.1624 | 2.86 | 543.1562, 303.0504, 287.0554, 129.0550, 85.0291 |

 

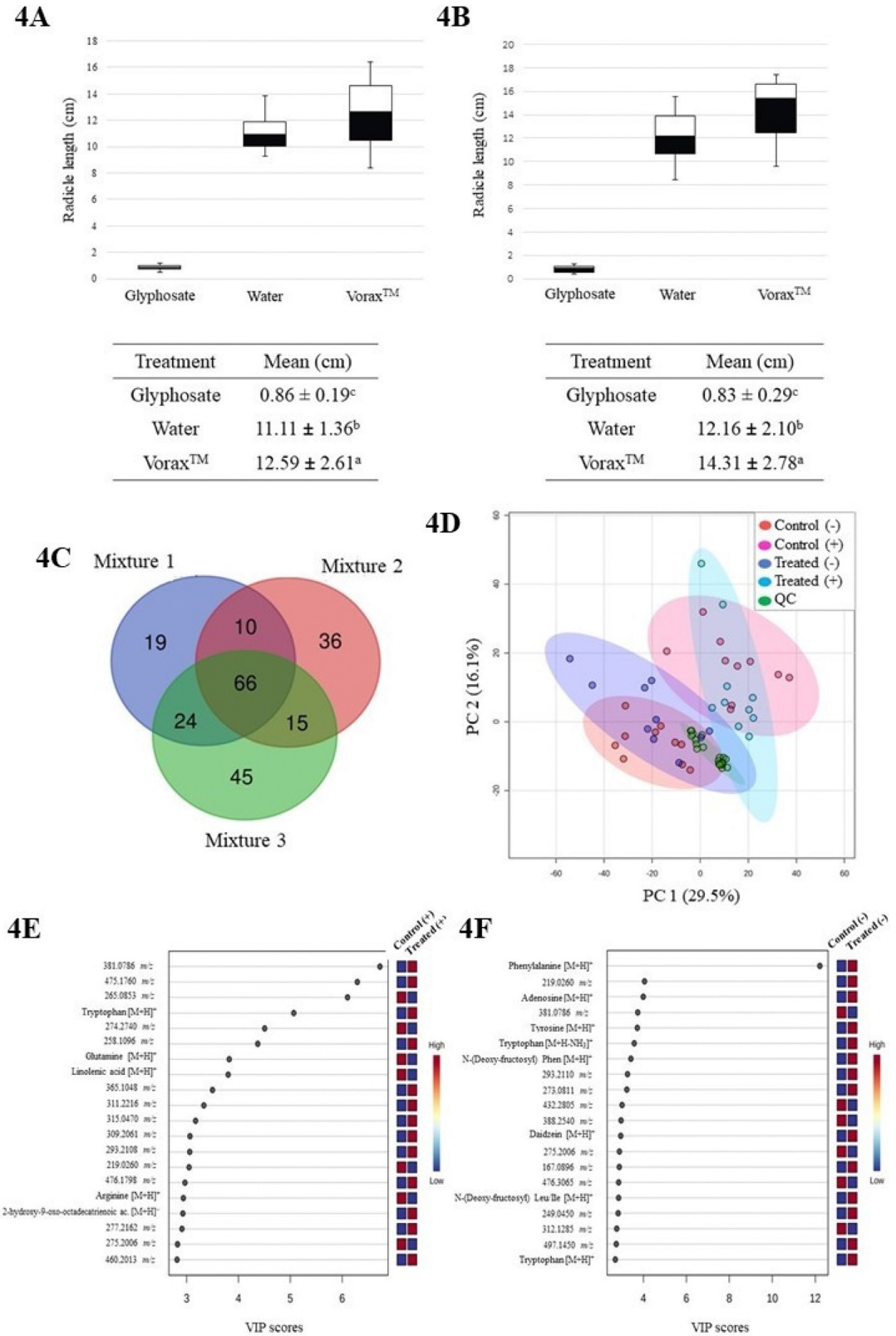


| Treatment | Mean (cm) |
|---|---|
| Glyphosate | 0.86 ± 0.19[c] |
| Water | 11.11 ± 1.36[b] |
| Vorax™ | 12.59 ± 2.61[a] |

| Treatment | Mean (cm) |
|---|---|
| Glyphosate | 0.83 ± 0.29[c] |
| Water | 12.16 ± 2.10[b] |
| Vorax™ | 14.31 ± 2.78[a] |

Fig. 4 Boxplots of radicle length measurement for *P. vulgaris* seed germination assays with (A) exposure of photoperiod 12 h/12 h light/dark (+) and (B) complete absence of sunlight (−). Values in the table are means of 20 replicates ± standard deviation (±SD). Different letters (a) and (b) indicate the statistically significant difference between trials ($p$-value $<0.05$). (C) Venn diagram with the distribution of annotated metabolites from seed extract of total absence of light assay (−) using mixture 1 (7 : 3, methanol : water, v/v), mixture 2 (3 : 1 : 1, chloroform : methanol : water, v/v) and mixture 3 (8 : 2, methanol : water with 0.1% formic acid, v/v). Metabolites were detected using the GNPS spectra library from the UHPLC-MS/MS data, positive mode, with $n$ = 5 (two repetitions). (D) PCA 2D scores plot (29.5% PC1 × 16.1% PC2), contribution of the first 15 variables in the projection (VIP scores) of the PLS-DA model (E) (+) data and (F) (−) data.

phenylalanine $[M + H]^+$ (*m/z* 166.0863), adenosine $[M + H]^+$ (*m/z* 268.1039), tyrosine $[M + H]^+$ (*m/z* 182.0811), tryptophan $[M + H - NH_3]^+$ (*m/z* 188.0707) and $[M + H]^+$ (*m/z* 205.0971), *N*-(1-deoxy-1-fructosyl) phenylalanine $[M + H]^+$ (*m/z* 328.1391), daidzein $[M + H]^+$ (*m/z* 255.0652) and *N*-(1-deoxy-1-fructosyl) leu/Ile $[M + H]^+$ (*m/z* 294.1545). By analysis, the most differentiated metabolite between groups was phenylalanine, with VIP score = 12.2. In addition, the amino acids tyrosine (VIP score = 3.9) and tryptophan (VIP score = 3.8) showed a significant increase in treated samples, indicating an alteration in the biosynthesis pathway of these compounds. All these metabolites were not detected in the biostimulant samples (Table A.2).

## 4. Discussion

So far, few studies have shown the Vorax™ biostimulant effects on the development, growth, and yield of crops. According to Röder *et al.* (2018), foliar treatment of *Solanum tuberosum* with Vorax™ promoted desirable effects, including leaves' senescence delay, changes in the chlorophyll content and yield gain. Besides, among a series of biostimulants evaluated for the development of *S. lycopersicum* L., only the plants subjected to the application of Vorax™ showed an increase in the dry mass of leaves compared to the control plants.[23] However, modulations in plant metabolism due to Vorax™ treatment were not evaluated yet. Given the importance of knowing the modes of action of biostimulants and their effects on plants, this study is the first to assess the specialized metabolism of a crop (*P. vulgaris*) after treatment with Vorax™.

Initially, the effect of foliar application of the biostimulant was investigated under ideal growing conditions. Our results demonstrated that the treatment significantly modified the metabolomic profile of *P. vulgaris* after three days. Increased levels of glutamic acid, nicotiflorin, the fatty acid 1-linolenoyl-glycerol, and its glycosylated derivatives 1-linolenoyl-3-galactopyranosyl glycerol and gingerglycolipid A, and a small decrease of rutin, were detected using untargeted metabolomics by UHPLC-MS/MS of the leaf extracts. Besides being the building blocks of proteins, the amino acid glutamic acid acts as a regulator of nitrogen metabolism (*i.e.*, Glutamine synthetase/glutamate–glutamine–oxoglutarate aminotransferase cycle) and it is a precursor of important metabolites such as GABA, a signaling molecule that plays versatile functions in the plant, commonly environmental responses.[39] 1-Linolenoylglycerol is a natural constituent of plants such as *Phaseolus vulgaris*,[4] mainly present in the root and cuticular waxes.[40,41] In particular, plant cuticular waxes offer protection against UV radiation, temperature changes, and mechanical damage, besides limiting water losses and gas exchange from the leaf epidermis.[42] The glycoglycerolipids, composed of a fatty acid chain, glycerol and hexose (galactose), play a fundamental role in several processes of recognition, adhesion and cell–cell and cell–environment communication,[43] but the specific biological function of the 1-linolenoyl-3-galactopyranosyl glycerol and gingerglycolipid A is not fully elucidated. Furthermore, accumulation of the flavonoid nicotiflorin, a glycosylated derivate of kaempferol, and decrease in the concentration level of rutin, a quercetin-*O*-glucoside, indicate modification of the shikimate pathway[44] that can be related to activation of plant protection mechanisms once flavonoids act in tolerance to oxidative stress,[45,46] playing important roles in the interaction between the plant and their environment.[47] These results suggest that the application of Vorax™ stimulates plant's tolerance response to environmental changes, modifying the biosynthesis pathway of amino acids, lipids and flavonoids.

The effect of Vorax™ biostimulant treatment under water stress growth conditions suggests an increase in the resilience of *P. vulgaris*. The analysis of the chlorophyll content showed an increase in the plants treated with the biostimulant after being submitted to stress (WST) compared to those only subjected to stress (WS) and not subjected to stress or treatment (NSNT). The increase in the chlorophyll content contributes to the improvement of plant tolerance once it is related to greater absorption and assimilation of nitrogen by the upregulation of the enzyme nitrate reductase that catalyzes the reduction of nitrate to nitrite, affecting the photosynthetic rate.[48]

By multivariate data analysis, an increase in the concentration of glutamic acid, 1-linolenoyl-3-galactopyranosyl glycerol and quercetin-3-*O*-xylopyranosyl-(1 → 6)-glucopyranoside was observed in the two trials subjected to water stress but more expressive with Vorax™ treatment (WST), what is similar to the data obtained in our previous assay. Once the plant's respiration process is highly compromised by the closing of stomata caused by the scarcity of water, we hypothesized that the triggering of glutamic acid production aids the nitrogen assimilation and increases chlorophyll content to regulate photosynthesis and, in association, cellular respiration. Thus, acting in the conservation and development of the plant.[39,49] Moreover, the increase in lipid production in WS and WST is probably related to the submission of plants to stress, since the literature reports the action of lipids in both defense and signaling mechanisms resulting from different stress conditions.[50] However, this effect is clearer in plants treated with Vorax™.

Another significant result was the decrease of the tryptophan and the 7-hydroxycoumarin productions in WS and NSNT. It may indicate the consumption of tryptophan as a precursor in the biosynthesis of specialized metabolites that act in protection and modulation of growth[17] and the involvement of coumarin in response to stress and treatment in aerial tissues, playing a primary role in plant health.[51]

Using the feature-based molecular networking (FBMN) tool we observed a flavonoid cluster with annotation of eight glycosylated flavonols, including quercetin-3-*O*-xylopyranosyl-(1 → 6)-glucopyranoside which was determined as a differential metabolite by the statistical analysis. The flavonoid cluster exhibited an accumulation of five quercetin derivates and two kaempferol derivates in WST samples in relation to WS and NSNT. Flavonoids are widely described as important specialized metabolites that regulate the plant's response to various environmental stimuli.[52] They act as signaling and precursor compounds in the biosynthesis of metabolites linked to defense mechanisms. Some flavonoids also have antioxidant

 

activity, inhibiting free radicals such as reactive oxygen species (ROS) induced by stress.[53] According to,[54] flavonols are probably the flavonoid class with the greatest participation in stress responses. In particular, quercetin 3-*O*-glycosides, which have a $C_6H_4(OH)_2$ catechol group on the B ring, are responsible for reducing various forms of ROS, compared to flavone and monohydroxy substituted glycosylated flavonols on the B ring.[55] The accumulation of flavonols in WST samples, mainly derived from quercetin 3-*O*-glycosides, seem to indicate that the application of Vorax™ induced the biosynthesis of flavonoids with antioxidant function, promoting tolerance of plant subjected to stress, thus indirectly stimulating the development of *P. vulgaris*.

In the evaluation of the influence of the biostimulant on seed germination, the highest mean in radicles length was exhibited for seeds treated with the biostimulant in relation to the control in both assays: with exposure of photoperiod 12 h/12 h light/dark (+) and in the complete absence of light (−). Furthermore, the mean radicle length for the seeds treated with Vorax™ obtained in the (−) assay, a value of 14.31 ± 2.78 cm, was higher than the mean of (+) assay, with a value of 12.59 ± 2.61 cm. This result suggests that even in the early stages of development, the biostimulant can act to improve plant performance, despite being subjected to the absence of luminosity.

To optimize the seed extraction method, three mixtures of solvents were tested. As expected, the number of annotations varied between solvent mixtures. In addition to the highest percentage of total annotations, mixture 3 also showed greater chemical diversity. Statistical analysis of (+) and (−) data, using mixture 3 as extracting solvent, presented mainly variations in amino acid concentration levels between Vorax™-treated and control groups. In particular, an increase in phenylalanine (Phe), tyrosine (Tyr), and tryptophan (Trp) levels after treatment, which are aromatic amino acids (AAAs) with a common precursor, chorismate, a product of the Shikimate pathway.[56,57]

In addition to the central role in the biosynthesis of proteins in all living cells, they play an important role in plant metabolism, acting as precursors of several natural products related to growth, development, defense, and protection.[58] Phe and Tyr are precursors to synthesize the phenylpropane base ($C_6C_3$) of many metabolites, including cinnamic acids, coumarins, and flavonoids. Trp is a precursor of several alkaloids, quinones, and phytoalexins,[56] such as indole-3-acetic acid which stimulates stretching cells, promoting the growth of roots and stems.[59] Previous studies indicate that the accumulation of these amino acids due to the application of biofertilizers and biostimulants, promotes several beneficial effects, depending on the plant species, product concentration and number of applications.[60] Commonly, the increase in the biosynthesis of these metabolites is associated with the stimulation of the plant's protection response,[8] providing evidence of how the biostimulant supports crop stress tolerance and development.

## 5. Conclusions

The use of products from biological sources has been demonstrated to be alternatives to conventional fertilizers and pesticides. In this study, *P. vulgaris* metabolome modulation due to the treatment of its leaves and seeds with the Vorax™ biostimulant under ideal and abiotic stress conditions was evaluated by untargeted metabolomics. Assessment of the development parameters of *P. vulgaris* treated with Vorax™ exhibited better results when subjected to abiotic stress (water deficient or the absence of luminosity), indicating the promising application of the biostimulant for crop recovery. Through UHPLC-MS in combination with multivariate statistical analysis and the molecular networking approach it was possible to annotate several metabolites whose concentration levels varied after biostimulant application, indicating that some biosynthetic pathways were modified by the treatment. Specifically, the accumulation of some lipids, amino acids, and flavonoids associated with plant stress tolerance was observed, showing that the biostimulant acts on the protection system. Considering that several regions will experience drier climate conditions in the future, the use of biostimulants may increase crop resilience, maintaining food security.

## Data availability

This study was carried out using publicly available data from Mass Spectrometry Interactive Virtual Environment (MassIVE) at **https://massive.ucsd.edu/ProteoSAFe/dataset.jsp?accession=MSV000092088** with accession number MSV000092088.

## Author contributions

Conceptualization, S. N. S., T. P. F. and R. L. N.; formal analysis, S. N. S., L. F. O. and L. D. B.; funding acquisition, T. P. F. and R. L. N.; investigation, S. N. S., L. F. O. and R. A. R.; methodology, S. N. S. and R. A. R.; resources, A. S. and F. P.; supervision, T. P. F.; validation, A. K. P. and A. S.; writing – original draft, S. N. S.; writing – review & editing, T. P. F., A. S. and F. P.; all authors reviewed the manuscript.

## Conflicts of interest

Stephanie Nemesio da Silva received a research grant from Tradecorp do Brasil Ltda. Luis Fernando de Oliveira received a research grant from Tradecorp do Brasil Ltda. Rodrigo Alberto Repke is an employee of Tradecorp do Brasil Ltda. Rafael Leiria Nunes is an executive director and shareholder in Tradecorp do Brasil Ltda. Taicia Pacheco Fill received from Tradecorp do Brasil Ltda earmarked funds for the aforementioned research grants. The remaining authors have no conflicts of interest to declare.

## Acknowledgements

The authors are grateful to Tradecorp do Brasil Comércio de Insumos Agrícolas Ltda [CNPJ 04.997.059/0003-19] for the financial support through the Fundação de Desenvolvimento da Unicamp (FUNCAMP) – [grant number 5447], Coordenação de Aperfeiçoamento de Pessoal de Nível Superior – Brasil (CAPES) – Finance Code 001, and Fundação de Amparo à

Pesquisa no Estado de São Paulo [grant number 2021/00728-0, 2022/02992-0]. In addition to funding agencies, the authors thank Dr Amadeu Hoshi Iglesias and Dr João Raul Belinato for instrumental analysis support.

## References

1 A. Pathania, S. K. Sharma and P. N. Sharma, *Broadening the Genetic Base of Grain Legumes*, Springer India, New Delhi, 2014, pp. 11–50.
2 IBGE, LSPA - Levantamento Sistemático da Produção Agrícola, **https://www.ibge.gov.br/estatisticas/economicas/agricultura-e-pecuaria/9201-levantamento-sistematico-da-producao-agricola.html?=&t=resultados**, (accessed May 22, 2022).
3 K. Ganesan and B. Xu, *Int. J. Mol. Sci.*, 2017, **18**, 2331.
4 I. David, M. D. Orboi, M. D. Simandi, C. A. Chirilă, C. I. Megyesi, L. Rădulescu, L. P. Drăghia, A. T. Lukinich-Gruia, C. Muntean, D. I. Hădărugă and N. G. Hădărugă, *PLoS One*, 2019, **14**, e0225474.
5 A. Saeid and K. Chojnacka, *Organic Farming*, Elsevier, 1[a], 2019, pp. 91–116.
6 N. O. Igiehon and O. O. Babalola, *Appl. Microbiol. Biotechnol.*, 2017, **101**, 4871–4881.
7 R. Anderson, P. E. Bayer and D. Edwards, *Curr. Opin. Plant Biol.*, 2020, **56**, 197–202.
8 B. Hamid, M. Zaman, S. Farooq, S. Fatima, R. Z. Sayyed, Z. A. Baba, T. A. Sheikh, M. S. Reddy, H. El Enshasy, A. Gafur and N. L. Suriani, *Sustainability*, 2021, **13**, 2856.
9 O. I. Yakhin, A. A. Lubyanov, I. A. Yakhin and P. H. Brown, *Front. Plant Sci.*, 2017, **7**, 1–32.
10 MarketsandMarkets, Biostimulants market, **https://www.marketsandmarkets.com/Market-Reports/biostimulant-market-1081.html?gclid=Cj0KCQjww4-hBhCtARIsAC9gR3bXllbyfXk4v-mLaQz-sr3vJSxZ1PWjParzmL7mrWZIwCW_L85Hrdu8aAkwZEALw_wcB**, (accessed March 30, 2023).
11 Y. Rouphael and G. Colla, *Front. Plant Sci.*, 2020, **11**, 40.
12 M. M. Posmyk and K. Szafrańska, *Front. Plant Sci.*, 2016, **7**, 1–6.
13 K. V. Supraja, B. Bunushree and P. Balasubramanian, *Ind. Crops Prod.*, 2020, **151**, 112453.
14 V. Walker, O. Couillerot, A. Von Felten, F. Bellvert, J. Jansa, M. Maurhofer, R. Bally, Y. Moënne-Loccoz and G. Comte, *Plant Soil*, 2012, **356**, 151–163.
15 D. Tiryaki, İ. Aydın and Ö. Atıcı, *Cryobiology*, 2019, **86**, 111–119.
16 U. B. Singh, D. Malviya, W. Khan, S. Singh, N. Karthikeyan, M. Imran, J. P. Rai, B. K. Sarma, M. C. Manna, R. Chaurasia, A. K. Sharma, D. Paul and J.-W. Oh, *Front. Plant Sci.*, 2018, **9**, 1–15.
17 R. Ben Mrid, B. Benmrid, J. Hafsa, H. Boukcim, M. Sobeh and A. Yasri, *Sci. Total Environ.*, 2021, **777**, 1–17.
18 L. Eggeling and M. Bott, *Handbook of Corynebacterium glutamicum*, CRC Press, 2005, vol. 3.
19 V. F. Wendisch, M. Bott, J. Kalinowski, M. Oldiges and W. Wiechert, *J. Biotechnol.*, 2006, **124**, 74–92.
20 Y. Wu, X. Jin, W. Liao, L. Hu, M. M. Dawuda, X. Zhao, Z. Tang, T. Gong and J. Yu, *Front. Plant Sci.*, 2018, **9**, 635.
21 J. Chen, Y. Wang, X. Guo, D. Rao, W. Zhou, P. Zheng, J. Sun and Y. Ma, *Biotechnol. Biofuels*, 2020, **13**, 41.
22 C. Röder, Á. F. Mógor, V. J. Szilagyi-Zecchin, L. G. Gemin and G. Mógor, *Comun. Sci.*, 2018, **9**, 211–218.
23 T. V. Silva, H. C. de Melo, M. F. de, C. Tarazi, L. C. Cunha Junior, L. F. C. Campos, A. dos, R. Nascimento, A. de and M. Catarino, *Emirates J. Food Agric.*, 2020, **32**, 255–262.
24 H. M. C. Marques, E. C. N. Cordeiro, J. de, O. Amatussi, G. B. de Lara, G. Mógor, L. C. B. M. Nedilha and Á. F. Mógor, *Res. Soc. Dev.*, 2021, **10**, e11101119377.
25 I. M. Rao, *The physiology of Vegetable Crops*, ed. H. Wien and H. C. Stützel, CAB international, London, UK, 2nd edn, 2020, pp. 271–285.
26 E. Silva, J. P. da Graça, C. Porto, R. Martin do Prado, C. B. Hoffmann-Campo, M. C. Meyer, E. de Oliveira Nunes and E. J. Pilau, *Sci. Rep.*, 2020, **10**, 138.
27 M. Almeida Trapp, G. D. De Souza, E. Rodrigues-Filho, W. Boland and A. Mithäöfer, *Front. Plant Sci.*, 2014, **5**, 417.
28 H. G. Gika, C. Zisi, G. Theodoridis and I. D. Wilson, *J. Chromatogr. B: Anal. Technol. Biomed. Life Sci.*, 2016, **1008**, 15–25.
29 T. Pluskal, S. Castillo, A. Villar-Briones and M. Orešič, *BMC Bioinf.*, 2010, **11**, 395.
30 J. Chong, O. Soufan, C. Li, I. Caraus, S. Li, G. Bourque, D. S. Wishart and J. Xia, *Nucleic Acids Res.*, 2018, **46**, W486–W494.
31 M. Wang, J. J. Carver, V. V. Phelan, L. M. Sanchez, N. Garg, Y. Peng, D. D. Nguyen, J. Watrous, C. A. Kapono, T. Luzzatto-Knaan, C. Porto, A. Bouslimani, A. V. Melnik, M. J. Meehan, W.-T. Liu, M. Crüsemann, P. D. Boudreau, E. Esquenazi, M. Sandoval-Calderón, R. D. Kersten, L. A. Pace, R. A. Quinn, K. R. Duncan, C.-C. Hsu, D. J. Floros, R. G. Gavilan, K. Kleigrewe, T. Northen, R. J. Dutton, D. Parrot, E. E. Carlson, B. Aigle, C. F. Michelsen, L. Jelsbak, C. Sohlenkamp, P. Pevzner, A. Edlund, J. McLean, J. Piel, B. T. Murphy, L. Gerwick, C.-C. Liaw, Y.-L. Yang, H.-U. Humpf, M. Maansson, R. A. Keyzers, A. C. Sims, A. R. Johnson, A. M. Sidebottom, B. E. Sedio, A. Klitgaard, C. B. Larson, C. A. Boya P, D. Torres-Mendoza, D. J. Gonzalez, D. B. Silva, L. M. Marques, D. P. Demarque, E. Pociute, E. C. O'Neill, E. Briand, E. J. N. Helfrich, E. A. Granatosky, E. Glukhov, F. Ryffel, H. Houson, H. Mohimani, J. J. Kharbush, Y. Zeng, J. A. Vorholt, K. L. Kurita, P. Charusanti, K. L. McPhail, K. F. Nielsen, L. Vuong, M. Elfeki, M. F. Traxler, N. Engene, N. Koyama, O. B. Vining, R. Baric, R. R. Silva, S. J. Mascuch, S. Tomasi, S. Jenkins, V. Macherla, T. Hoffman, V. Agarwal, P. G. Williams, J. Dai, R. Neupane, J. Gurr, A. M. C. Rodríguez, A. Lamsa, C. Zhang, K. Dorrestein, B. M. Duggan, J. Almaliti, P.-M. Allard, P. Phapale, L.-F. Nothias, T. Alexandrov, M. Litaudon, J.-L. Wolfender, J. E. Kyle, T. O. Metz, T. Peryea, D.-T. Nguyen, D. VanLeer, P. Shinn, A. Jadhav, R. Müller, K. M. Waters, W. Shi, X. Liu, L. Zhang, R. Knight, P. R. Jensen, B. Ø. Palsson, K. Pogliano,

 

R. G. Linington, M. Gutiérrez, N. P. Lopes, W. H. Gerwick, B. S. Moore, P. C. Dorrestein and N. Bandeira, *Nat. Biotechnol.*, 2016, **34**, 828–837.

32 L.-F. Nothias, D. Petras, R. Schmid, K. Dührkop, J. Rainer, A. Sarvepalli, I. Protsyuk, M. Ernst, H. Tsugawa, M. Fleischauer, F. Aicheler, A. A. Aksenov, O. Alka, P.-M. Allard, A. Barsch, X. Cachet, A. M. Caraballo-Rodriguez, R. R. Da Silva, T. Dang, N. Garg, J. M. Gauglitz, A. Gurevich, G. Isaac, A. K. Jarmusch, Z. Kameník, K. Bin Kang, N. Kessler, I. Koester, A. Korf, A. Le Gouellec, M. Ludwig, C. Martin H., L.-I. McCall, J. McSayles, S. W. Meyer, H. Mohimani, M. Morsy, O. Moyne, S. Neumann, H. Neuweger, N. H. Nguyen, M. Nothias-Esposito, J. Paolini, V. V. Phelan, T. Pluskal, R. A. Quinn, S. Rogers, B. Shrestha, A. Tripathi, J. J. J. van der Hooft, F. Vargas, K. C. Weldon, M. Witting, H. Yang, Z. Zhang, F. Zubeil, O. Kohlbacher, S. Böcker, T. Alexandrov, N. Bandeira, M. Wang and P. C. Dorrestein, *Nat. Methods*, 2020, **17**, 905–908.

33 J. Godzien, A. Gil de la Fuente, A. Otero and C. Barbas, *Compr. Anal. Chem.*, 2018, 415–445.

34 R. Ekman, J. Silberring and A. Westman-Brinkmalm, Ann M. Kraj, *Mass spectrometry instrumentation, interpretation, and applications*, John Wiley & Sons, Inc., 2010, vol. 21.

35 B. Thiele, N. Stein, M. Oldiges and D. Hofmann, *Amino acids analysis*, Humana Press, 828th edn, 2012, pp. 317–328.

36 S. Y. Park, J. S. Kim, S. Y. Lee, K. Bae and S. S. Kang, *Nat. Prod. Sci.*, 2008, **14**, 281–288.

37 C. Cavaliere, F. Cucci, P. Foglia, C. Guarino, R. Samperi and A. Laganà, *Rapid Commun. Mass Spectrom.*, 2007, **21**, 2177–2187.

38 A. Steckel and G. Schlosser, *Molecules*, 2019, **24**, 611.

39 S. Okumoto, D. Funck, M. Trovato and G. Forlani, *Front. Plant Sci.*, 2016, **7**, 1–3.

40 R. Simões, A. Rodrigues, S. Ferreira-Dias, I. Miranda and H. Pereira, *Plants*, 2020, **9**, 1165.

41 Y.-C. Chien, C.-H. Lin, M. Y. Chiang, H.-S. Chang, C.-H. Liao, I.-S. Chen, C.-F. Peng and I.-L. Tsai, *Phytochemistry*, 2012, **80**, 50–57.

42 T. Shepherd and D. Wynne Griffiths, *New Phytol.*, 2006, **171**, 469–499.

43 H. E. Carter, P. Johnson and E. J. Weber, *Annu. Rev. Biochem.*, 1965, **34**, 109–142.

44 R. A. Dixon and N. L. Paiva, *The Plant Cell*, 1995, **7**, 1085–1097.

45 M. Ren, Z. Wang, M. Xue, X. Wang, F. Zhang, Y. Zhang, W. Zhang and M. Wang, *PLoS One*, 2019, **14**, e0224296.

46 A. A. Fortunato, L. Araujo and F. A. Rodrigues, *J. Phytopathol.*, 2016, **165**, 131–142.

47 L. Pourcel, J. M. Routaboul, V. Cheynier, L. Lepiniec and I. Debeaujon, *Trends Plant Sci.*, 2007, **12**, 29–36.

48 A. S. Al-Erwy, A. Al-Toukhy and S. O. Bafeel, *Int. J. Adv. Res. Biol. Sci.*, 2016, **3**, 296–310.

49 G. Franzoni, G. Cocetta and A. Ferrante, *Physiol. Mol. Biol. Plants*, 2021, **27**, 1059–1072.

50 J. L. Harwood, *Lipids in Photosynthesis: Structure, Function and Genetics*, Springer, 6th edn, 1998, pp. 287–302.

51 K. Robe, E. Izquierdo, F. Vignols, H. Rouached and C. Dubos, *Trends Plant Sci.*, 2021, **26**, 248–259.

52 L. Lepiniec, I. Debeaujon, J.-M. Routaboul, A. Baudry, L. Pourcel, N. Nesi and M. Caboche, *Annu. Rev. Plant Biol.*, 2006, **57**, 405–430.

53 B. Winkel-Shirley, *Curr. Opin. Plant Biol.*, 2002, **5**, 218–223.

54 S. Pollastri and M. Tattini, *Ann. Bot.*, 2011, **108**, 1225–1233.

55 G. Agati, C. Brunetti, A. Fini, A. Gori, L. Guidi, M. Landi, F. Sebastiani and M. Tattini, *Antioxidants*, 2020, **9**, 1098.

56 P. M. Dewick, *Medicinal Natural Products: A byosynthetic Approach*, John Wiley & Sons, Ltd, Chichester, UK, 3rd edn, 2009.

57 V. Tzin and G. Galili, *Mol. Plant*, 2010, **3**, 956–972.

58 H. Maeda and N. Dudareva, *Annu. Rev. Plant Biol.*, 2012, **63**, 73–105.

59 E. Tanimoto, *CRC. Crit. Rev. Plant Sci.*, 2005, **24**, 249–265.

60 R. Bulgari, G. Cocetta, A. Trivellini, P. Vernieri and A. Ferrante, *Biol. Agric. Hortic.*, 2015, **31**, 1–17.